there is no tendency for spin coupling, that for intermediate ranges of distances (2.49 to 2.82 A) the coupling is antiparallel and for the long distances ($\geq$2.96 A) parallel spin coupling occurs. If a group of atoms occurs in a spatial arrangement such that no physically consistent assignment of moments can be made, it seems that no moment alignment among these atoms will occur. Not only the antiferromagnetic structure of α-Mn but the absence of a magnetic structure for β-Mn are understandable on the basis of these statements.

While it is not possible to specify exactly the magnitude of the moments of the respective atoms in α-Mn, it is established that they are well above the value of 0.5 μ_B that is given in the literature.

No significant deviation from the accepted crystal structure descriptions of both α- and β-Mn could be detected in the neutron diffraction results.

ACKNOWLEDGMENTS

We acknowledge gratefully the many contributions of Mr. R. Waterstrat to this investigation—the preparation of materials, the measurement and calculation of intensities, and the x-ray diffraction work. Also, we acknowledge with pleasure the helpful discussions on questions of magnetism with Dr. C. P. Bean and Dr. I. Jacobs and we are indebted to them for the magnetic measurements. We are equally grateful for the suggestions and help of Mrs. B. Decker, especially for the loan of the coordination figures constructed by her.

PHYSICAL REVIEW VOLUME 101, NUMBER 2 JANUARY 15, 1956

Galvanomagnetic Effects in Bismuth*

B. ABELES AND S. MEIBOOM
Department of Applied Mathematics, The Weizmann Institute of Science, Rehovot, Israel

(Received August 15, 1955)

Conductivity, Hall effect, and magnetoresistance in single crystals of pure and tin-doped bismuth have been measured as functions of temperature between 80 and 300°K and as functions of magnetic field up to 2000 oersted. A simple many-valley model for the band structure of bismuth is proposed, and explicit expressions for the galvanomagnetic effects are derived. Numerical values are obtained for the number of conduction electrons and holes, their mobilities, and the overlap of valence and conduction bands.

I. INTRODUCTION

THE galvanomagnetic effects in single crystals of bismuth have been studied extensively.[1–6] An attempt to explain the observed facts in terms of band structure has been made by Jones.[7] This author calculated the galvanomagnetic effects on the assumption that the band structure of bismuth can be approximated by a simple model. However, the model adopted by Jones leads to results which are partially at variance with experiment. For instance, the longitudinal magnetoresistance in the direction of any of the crystallographic axes is calculated to be zero, while experimentally the longitudinal effect is of the same order of magnitude as the transverse effect. The theory is also unable to explain the pronounced anisotropy of the transverse effects at strong magnetic fields. In this paper we will show that a somewhat different model leads to much better agreement between calculated and experimental values.

Measurements of galvanomagnetic effects in different crystallographic directions in weak magnetic fields and at temperatures between 80 and 300°K have been carried out, as the data available in the literature were considered to be insufficient for a satisfactory test of the theory. We have also measured the galvanomagnetic effects in tin-doped bismuth. Thomson[8,9] has reported that small additions of tin to bismuth act in many ways analogously to the addition of acceptor elements to semiconductors, and it should thus be possible to obtain from these measurements more direct information as to the relative contributions of the valence and the conduction bands to the conductivity.

II. EXPERIMENTAL

Single crystals of bismuth were prepared from spectroscopically pure bismuth, supplied by Johnson and Mathey, specified to be better than 99.996% pure. The method used in growing the single crystals follows closely one of the techniques described by Kapitza.[10] The single crystals obtained had the shape of rods with nearly circular cross section of diameter between 1 and 2 mm. Rods of any specified crystallographic direction

* Part of a dissertation submitted by B. Abeles to the Hebrew University, Jerusalem, in partial fulfillment of the requirements for the degree of Doctor of Philosophy.

[1] P. Kapitza, Proc. Roy. Soc. (London) **A119**, 358 (1928).
[2] O. Steirstadt, Z. Physik **95**, 355 (1935).
[3] de Haas, Blom, and Schubnikov, Physica **2**, 907 (1935).
[4] A. N. Gerritzen and W. J. de Haas, Physica **8**, 802 (1940).
[5] Gerritzen, de Haas, and van der Star, Physica **9**, 241 (1942).
[6] Y. Tanabe, Science Repts. Insts. Tohoku Univ. **A2**, 341 (1950).
[7] H. Jones, Proc. Roy. Soc. (London) **A155**, 653 (1936).
[8] N. Thomson, Proc. Roy. Soc. (London) **A155**, 111 (1936).
[9] N. Thomson, Proc. Roy. Soc. (London) **A164**, 24 (1938).
[10] An adaptation of the "plate furnace" method described in reference 1 was used.

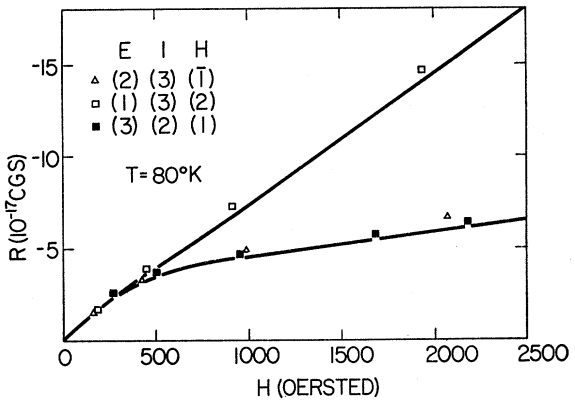

FIG. 1. Hall field as a function of magnetic field strength at 80°K. The points indicate experimental values; the curves were calculated from Eq. (12), using the values of the parameters given in Table II. The directions of the current **I**, the magnetic field **H**, and the observed component of the electric field **E** are given in the figure. (3) denotes the trigonal axis, (1) a binary axis and (2) indicates the direction perpendicular to (1) and (3).

could be obtained by the use of seeds.[1] The crystallographic directions of the rods were determined with the help of the principal cleavage plane. It was found that the cleaving was done best while the crystal was immersed in liquid nitrogen. At low temperatures the crystal is brittle and cleaves without any deformation.

Crystals of three orientations were grown: with the rod axis parallel to the trigonal axis, with the rod axis parallel to a binary axis and with the rod axis perpendicular to the trigonal axis and one of the binary axes. Absence of twinning was checked by etching the rods in a saturated aqueous solution of KI to which some iodine was added.

By the same procedure, a number of bismuth rods containing small additions of tin were prepared (up to 0.2 weight percent). The tin content was obtained by spectroscopic analysis of the samples after completion of the electrical measurements. This procedure was necessary, because appreciable segregation of tin takes place during crystallization.

Samples of about 8 mm length were cut from the single crystal rods. Current leads were soldered to the ends of the sample. Silver potential leads (of diameter 0.05 mm) were welded to the sample by condensor discharge.[1] The dimensions of the rod and the distance between the potential probes were determined with a travelling microscope.

The resistance and Hall effect were measured on a number of samples as functions of the magnetic field up to about 2000 oersted, and as functions of temperature between liquid nitrogen temperature and room temperature. An ac method similar to the one described by Donoghue and Earthy[11] was used. It was found advantageous to modify the apparatus described in reference 11, by the addition of a phase detector.[12] This made it possible to dispense with the phase shifter and filter used in the original method.

In Figs. 1, 2, and 3 results for the Hall field R and the magnetoresistance Q at 80°K are given as functions of magnetic field.[13] The measurements were carried out on a number of differently oriented crystals and for various directions of the magnetic field. The direction of the current **I**, the direction of the magnetic field **H** and the direction of the measured component of the electric field **E** are indicated in the figures. Similar curves for 300°K show no appreciable saturation at 2000 oersted.

In Table I are given the values for the specific conductivity, the Hall coefficient, and the magnetoresistance coefficient at 80°K and 300°K. The coefficients were obtained by graphical extrapolation of the measured values to zero magnetic field. In this table those coefficients which should be equal because of crystal symmetry[14,15] have been taken together. In fact, the measured values for these coefficients coincided within the experimental accuracy, and the values given in the table are averages.

The samples containing additions of tin show a

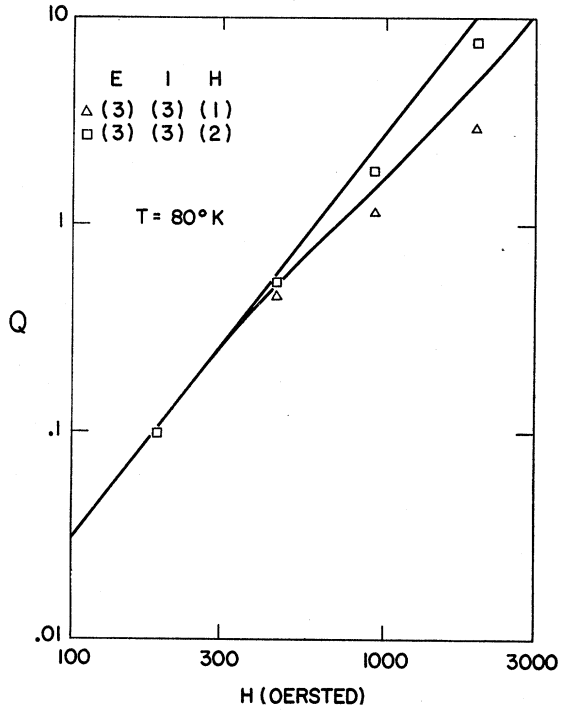

FIG. 2. Magnetoresistance as a function of magnetic field strength at 80°K. The curves have been calculated from Eq. (13). Other details as for Fig. 1.

[11] J. J. Donoghue and W. P. Earthy, Rev. Sci. Instr. **22**, 513 (1951).

[12] N. A. Schuster, Rev. Sci. Instr. **22**, 254 (1951).

[13] We will use the term magnetoresistance for the quantity $Q=(\rho_H-\rho_0)/\rho_0$, where ρ_H is the resistance of the sample in magnetic field H and ρ_0 the resistance in zero magnetic field. The term magnetoresistance coefficient will be used for the quantity $q=\lim(Q/H^2)$ as $H\to 0$. Similarly, we will denote by Hall field the quantity R, which is related to the Hall coefficient r by: $r=\lim(R/H)$ as $H\to 0$.

[14] D. Shoenberg, Proc. Cambridge Phil. Soc. **31**, 265 (1935).

[15] D. Shoenberg, Proc. Cambridge Phil. Soc. **31**, 271 (1935).

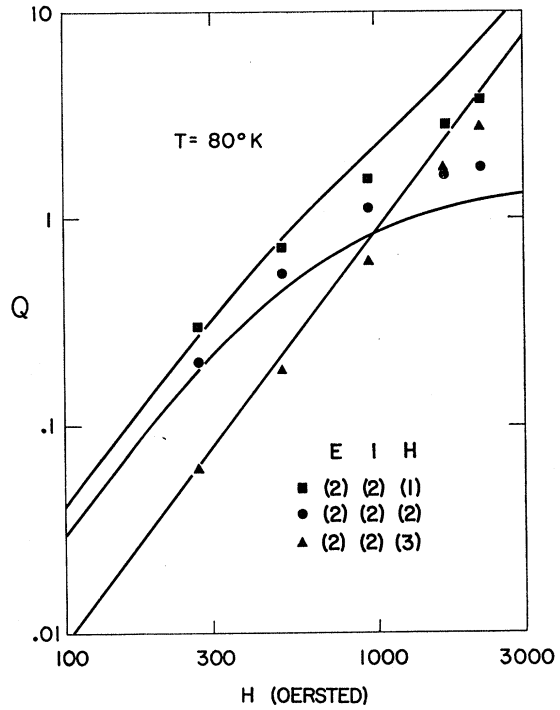

FIG. 3. Magnetoresistance as a function of magnetic field strength at 80°K. The curves have been calculated from Eq. (13). Other details as for Fig. 1.

peculiar dependence of resistance and galvanomagnetic coefficients on temperature. Some of the measurements are given in Figs. 4, 5, and 6. Similar results were obtained by Thomson.[8,9] A discussion of this behavior will be given in Sec. IV.B.

III. THEORY

The physical properties of bismuth indicate that in this metal there is a small overlap of the conduction band and valence band[7,16] and that electrical conductivity is due to a small number of electrons at the bottom of the conduction band and an equal number of holes at the top of the valence band. The galvanomagnetic effects are thus determined by the detailed structure of the bottom of the conduction band and of the top of the valence band. In the absence of theoretical calculations of the band structure of bismuth, the following model will be assumed:

(1) The energy extrema of interest are nondegenerate. We can then use the usual approximation for the energy $\mathcal{E}$ as a function of crystal momentum $\mathbf{P}$

$$\mathcal{E}=\pm[(P_1^2/2m_1)+(P_2^2/2m_2)+(P_3^2/2m_3)]. \quad (1)$$

(2) According to assumption 1, the energy surfaces near an extremum are sets of ellipsoids. A number of these sets must be arranged in momentum space in accordance with the rhombohedral symmetry of the bismuth crystal. The two simplest cases which fulfill this requirement are:

(a) One set of ellipsoids of revolution with the axis of revolution parallel to the trigonal axis of the crystal.

(b) Three sets of ellipsoids, each set having one of its axes parallel to the trigonal axis and another axis parallel to a binary axis. (One set transforms into another by rotation of 120° about the trigonal axis.) Case (a) will be adopted for the valence band and case (b) for the conduction band.

(3) The relaxation time of the electrons and of the holes is independent of energy. This assumption is a fair approximation at low temperatures where the statistics is nearly degenerate. It will also be used at higher temperatures, because of lack of more specific information on the dependence of relaxation time on $\mathbf{P}$.

It appears that other reasonable assumptions for the relaxation time will not change the essential results of

TABLE I. Comparison of measured and calculated conductivity and weak magnetic field galvanomagnetic coefficients. λ_{ik} denotes the conductivity tensor, $r_{ik}(l)$ the Hall coefficient and $q_{ik}(l)$ the magnetoresistance coefficient. The index i indicates the observed component of the electric field, k the direction of the current and l the direction of the magnetic field. (3) denotes the trigonal axis, (1) a binary axis, and (2) is perpendicular to (1) and (3). The calculated values were obtained from Eqs. (14) for the values of the parameters of Table II. All quantities in cgs units.

	300°K calc.	300°K exp.	80°K calc.	80°K exp.
$\lambda_{11}, \lambda_{22}\times10^{-16}$	0.76	0.75	2.7	2.5
$\lambda_{33}\times10^{-16}$	0.68	0.60	2.4	2.4
$-r_{31}(2), r_{13}(2), -r_{23}(1), r_{32}(1)\times10^{20}$	−1.7	−1.5	−9.2	−9.3
$-r_{12}(3), r_{21}(3)\times10^{20}$	0.19	0.05	0.66	0.3[a]
$q_{11}(1), q_{22}(2)\times10^{8}$	0.89	0.78	280	290
$q_{11}(2), q_{22}(1)\times10^{8}$	1.3	1.3	400	450
$q_{11}(3), q_{22}(3)\times10^{8}$	0.36	0.27	90	80
$q_{33}(1), q_{33}(2)\times10^{8}$	1.1	1.3	320	330
$q_{33}(3)\times10^{8}$	0	0.1	0	30

[a] The sample was accidentally destroyed before this measurement could be taken. The value quoted is taken from Thomson[9] and is for 90°K.

[16] H. Jones, Proc. Roy. Soc. (London) **A147**, 396 (1934).

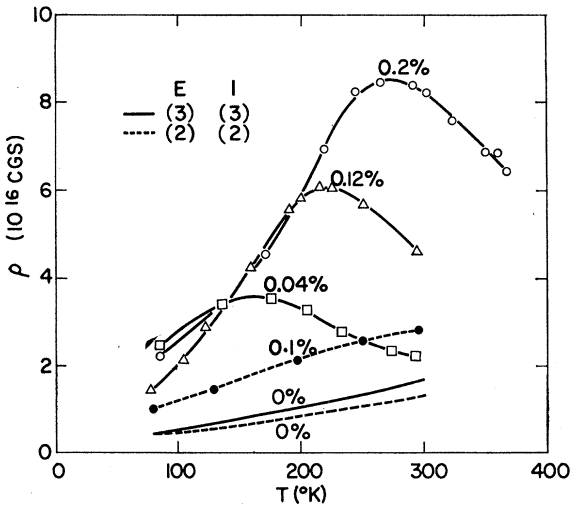

FIG. 4. Measured specific resistance of tin-doped bismuth as a function of temperature. The tin content in weight percent is indicated in the figure. The solid lines give the resistance in the direction of the trigonal axis, the dashed lines the resistance in a direction perpendicular to the trigonal axis.

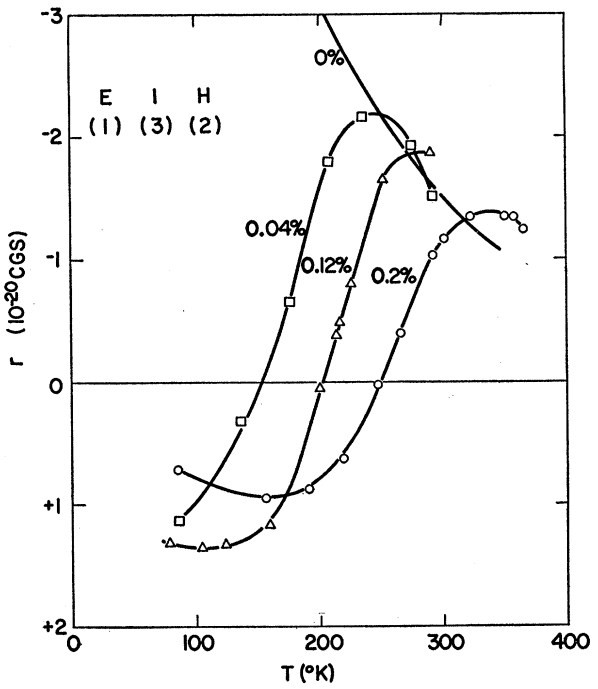

FIG. 5. Measured Hall coefficient of tin-doped bismuth as a function of temperature. The tin content in weight percent is indicated in the figure. Current parallel to trigonal axis.

the theory. This can be understood from the fact that the large galvanomagnetic effects in bismuth are a result of the presence of more than one carrier, while the dependence of the relaxation time on **P** gives only a minor contribution.

(4) In the relaxation processes only transitions between states belonging to the same extremum take place. With this assumption, each extremum can be treated independently, the total current being given as the sum of the contributions from each extremum.

The only difference between the above model and the one treated by Jones is the adoption of case (b) instead of case (a) for the conduction band. It should be noted that a model for the conduction band essentially equivalent to case (b) has been assumed by Shoenberg[17] in a theoretical interpretation of the de Haas-van Alphen effect in bismuth.

The calculation of the galvanomagnetic effects for the above model can be carried out in a way similar to the one given for germanium in a previous paper.[18] However, the assumption that the relaxation time is independent of **P** allows considerable simplification. For this case, the following equation can be derived for the current density contribution **i** of one extremum[19]:

$$i_i=\sum_k \sigma_{ik}[\mathbf{E}+(1/enc)\mathbf{i}\times\mathbf{H}]_k, \qquad (2)$$

where **E** is the electric field, **H** the magnetic field, e the charge of the electron (to be taken negative in the case of electrons and positive in the case of holes), c the velocity of light, n the number of carriers near the energy extremum per unit volume of the crystal. The components of the tensor σ_{ik}, referred to the principal axes are given by

$$\sigma_{ik}=(e^2n\tau/m_i)\delta_{ik}=en\mu_i\delta_{ik}, \qquad (3)$$

where τ is the relaxation time and δ_{ik} the Kronecker symbol. μ_i can be regarded as the mobility of the charge carrier in the i direction. Since these mobilities refer to charge carriers belonging to one extremum, we will refer to them as "partial mobilities."

Solving Eq. (2) for **i**, one obtains

$$i_i=\sum_k s_{ik}E_k, \qquad (4)$$

where s_{ik} are the expressions

$$\begin{aligned} s_{11}&=G\mu_1[1+(\mu_2\mu_3H_1^2/c^2)],\\ s_{12}&=G\mu_1\mu_2[(H_3/c)+(\mu_3H_1H_2/c^2)],\\ s_{ik}(\mathbf{H})&=s_{ki}(-\mathbf{H}),\\ G&=en\{1+[(\mu_2\mu_3H_1^2+\mu_3\mu_1H_2^2\\ &\qquad +\mu_1\mu_2H_3^2)/c^2]\}^{-1}. \end{aligned} \qquad (5)$$

The other components of s_{ik} are obtained by cyclic permutation of the indices. The set s_{ik} can be interpreted as a tensor characterising the conductivity contribution of one extremum. The expressions (5) are the components of this tensor referred to a coordinate

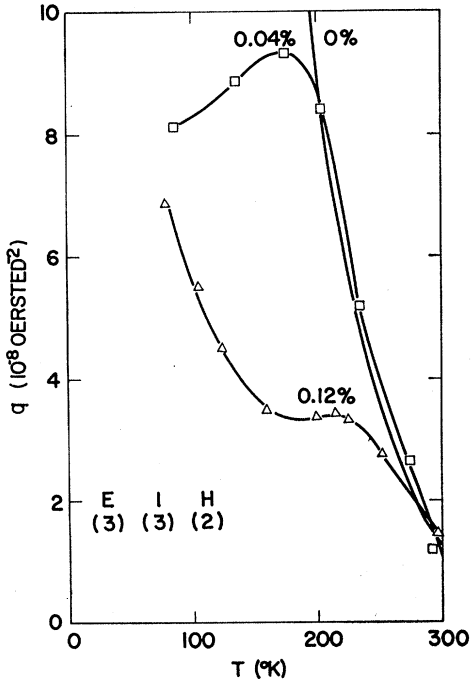

FIG. 6. Measured transverse magnetoresistance coefficient of tin-doped bismuth as a function of temperature. Details as in Fig. 5.

[17] D. Shoenberg, Proc. Roy. Soc. (London) **A170**, 341 (1939).
[18] B. Abeles and S. Meiboom, Phys. Rev. **95**, 31 (1954).
[19] See A. H. Wilson, *The Theory of Metals* (Cambridge University Press, Cambridge, 1953), second edition, p. 225. Substitution of Eq. (8.551.1) into (8.551.4), followed by partial integration, gives the desired result.

system along the principal axes of the energy ellipsoids. We next have to sum the current contributions of all the extrema. In order to carry out this summation, we first have to refer the tensors s_{ik} belonging to the different extrema to a common coordinate system. We shall use a right-handed orthogonal coordinate system such that the 1-axis is along a binary axis of the crystal and the 3-axis along the trigonal axis. This coordinate system is along the principal axes of the energy ellipsoids describing the top of the valence band [case (a)] and along the principal axis of one of the three sets of ellipsoids describing the bottom of the conduction band [case (b)]. For these extrema the components of s_{ik} are given directly by Eq. (5). For the other two conduction band extrema, we have to apply the following transformation to s_{ik}:

$$A_{i'}{}^{i}=\tfrac{1}{2}\begin{vmatrix}-1 & \pm\sqrt{3} & 0\\ \mp\sqrt{3} & -1 & 0\\ 0 & 0 & 2\end{vmatrix}. \tag{6}$$

This transformation expresses rotations of $\pm 120°$ about the 3-axis. Calculating

$$s_{i'k'}=\sum_{i,k} A_{i'}{}^{i}A_{k'}{}^{k}s_{ik}, \tag{7}$$

and substituting in s_{ik}

$$\begin{aligned}H_1&=-(1/2)H_{1'}\mp(\sqrt{3}/2)H_{2'},\\ H_2&=\pm(\sqrt{3}/2)H_{1'}-(1/2)H_{2'},\\ H_3&=H_{3'},\end{aligned} \tag{8}$$

we obtain

$$\begin{aligned}
s_{1'1'}&=g[\mu_1+3\mu_2+(4\mu_1\mu_2\mu_3H_{1'}{}^2/c^2)],\\
s_{2'2'}&=g[3\mu_1+\mu_2+(4\mu_1\mu_2\mu_3H_{2'}{}^2/c^2)],\\
s_{3'3'}&=4g[\mu_3+(\mu_1\mu_2\mu_3H_{3'}{}^2/c^2)],\\
s_{1'2'}&=g[\pm\sqrt{3}(\mu_1-\mu_2)+(4\mu_1\mu_2H_{3'}/c)\\
&\qquad+(4\mu_1\mu_2\mu_3H_{1'}H_{2'}/c^2)],\\
s_{2'3'}&=(g\mu_3/c)[(3\mu_1+\mu_2)H_{1'}\mp\sqrt{3}(\mu_1-\mu_2)H_{2'}\\
&\qquad+(4\mu_1\mu_2H_{2'}H_{3'}/c)],\\
s_{3'1'}&=(g\mu_3/c)[(\mu_1+3\mu_2)H_{2'}\mp\sqrt{3}(\mu_1-\mu_2)H_{1'}\\
&\qquad+(4\mu_1\mu_2H_{3'}H_{1'}/c)],\\
g&=(en/4)\{1+(1/4c^2)[\mu_3(3\mu_1+\mu_2)H_{1'}{}^2\\
&\qquad+\mu_3(\mu_1+3\mu_2)H_{2'}{}^2+4\mu_1\mu_2H_{3'}{}^2\\
&\qquad\pm2\sqrt{3}\mu_3(\mu_1-\mu_2)H_{1'}H_{2'}]\}^{-1}.
\end{aligned} \tag{9}$$

We can now sum the current contributions of the four extrema. The result has the form

$$I_i=\sum_k S_{ik}E_k, \tag{10}$$

where $\mathbf{I}$ is the total current density and S_{ik} is the sum of the following terms: expression (5) for the holes (with e positive), expression (5) for the electrons of one of the conduction band minima (with e negative) and expression (9), once with the upper and once with the lower sign for the other two conduction band minima.

In the usual experimental arrangement for measuring the galvanomagnetic effects, the current density $\mathbf{I}$ and magnetic field $\mathbf{H}$ are given, and the component of $\mathbf{E}$ in a specified direction is measured. The galvanomagnetic effects are thus not given directly by the coefficients in Eq. (10), but rather by the coefficients in

$$E_i=\sum_k R_{ik}I_k. \tag{11}$$

Although the calculation of $R_{ik}(\mathbf{H})$ is straightforward, the expressions obtained are rather cumbersome for the general case. We will give here explicit equations only for the cases where $\mathbf{H}$ is along either the 1-axis (binary axis), the 2-axis, or the 3-axis (trigonal axis). In order to differentiate between these cases, we will write $R_{ik}(l)$ where l denotes the direction of the magnetic field. For these cases we obtain

$$R_{ik}(l)=r_{ik}(l)H[1+a_{ik}(l)H^2][1+b_{ik}(l)H^2+c_{ik}(l)H^4]^{-1},\quad i\neq k\neq l\neq i \tag{12}$$

$$Q_{ik}(l)\equiv\lambda_{ik}R_{ik}(l)-1=q_{ik}(l)H^2[1+d_{ik}(l)H^2]\times[1+e_{ik}(l)H^2+f_{ik}(l)H^4]^{-1},\quad i=k. \tag{13}$$

Equations (12) and (13) give the Hall field and magnetoresistance respectively.[13] Below are given the expressions for $r_{ik}(l)$ and $q_{ik}(l)$ for arbitary N and P. ($N=3n$ is the total number of electrons and P the total number of holes per unit volume.) The expressions for the other coefficients in (12) and (13) are cumbersome for the general case ($N\neq P$) and we shall give them only for $N=P$.

$$\begin{aligned}
\lambda_{11}&=(e/2)[N(\mu_1+\mu_2)+2P\nu_1],\\
\lambda_{33}&=e[N\mu_3+P\nu_3],\\
r_{12}(3)&=-r_{21}(3)=(e/c\lambda_{11}{}^2)(N\mu_1\mu_2-P\nu_1{}^2),\\
r_{23}(1)&=-r_{32}(1)=r_{31}(2)=-r_{13}(2)\\
&\qquad=(e/2c\lambda_{11}\lambda_{33})[N(\mu_1+\mu_2)\mu_3-2P\nu_1\nu_3],\\
q_{11}(1)&=(eN/8c^2\lambda_{11})\mu_3(\mu_1-\mu_2)^2,\\
q_{11}(2)&=(eN\mu_3/8c^2\lambda_{11}\lambda_{33})[\lambda_{33}(\mu_1-\mu_2)^2\\
&\qquad+2eP\nu_3(\mu_1+\mu_2+2\nu_3)^2],\\
q_{11}(3)&=(e^2N/4c^2\lambda_{11}{}^2)\{N\mu_1\mu_2(\mu_1-\mu_2)^2\\
&\qquad+2P\nu_1[(\mu_1+\mu_2)(\mu_1\mu_2+\nu_1{}^2)+4\mu_1\mu_2\nu_1]\},\\
q_{33}(1)&=(e^2/2c^2\lambda_{11}\lambda_{33})NP\nu_1(\mu_1+\mu_2)(\mu_3+\nu_3)^2,\\
q_{33}(3)&=0,
\end{aligned} \tag{14}$$

$$a_{31}(2)=a_{13}(2)=\frac{\mu_3[\mu_1\mu_3(\mu_1+3\mu_2)-\nu_1\nu_3(3\mu_1+\mu_2)]}{2c^2[\mu_3(\mu_1+\mu_2)-2\nu_1\nu_2]},$$

$$a_{12}(3)=\mu_1\mu_2/c^2,$$

$$d_{11}(2)=\frac{\mu_3\nu_3(\mu_1+\mu_2+2\nu_1)[\nu_1(3\mu_1+\mu_2)+\mu_1(\mu_1+3\mu_2)]}{c^2\{\mu_3(\mu_1-\mu_2)^2+\nu_3[8\nu_1(\mu_1+\mu_2+\nu_1)+3\mu_1^2+2\mu_1\mu_2+3\mu_2^2]\}},$$

$$d_{11}(3)=\frac{\mu_1\mu_2\nu_1[\nu_1(\mu_1+\mu_2)+2\mu_1\mu_2](\mu_1+\mu_2+2\nu_1)}{c^2\{\mu_1\mu_2(\mu_1-\mu_2)^2+2\nu_1[\mu_1\mu_2(\mu_1+\mu_2)+4\mu_1\mu_2\nu_1+\nu_1^2(\mu_1+\mu_2)]\}}, \tag{15}$$

$$d_{33}(2)=\mu_1\mu_3(\mu_1+3\mu_2)/2c^2(\mu_1+\mu_2),$$

$$b_{31}(2)=b_{13}(2)=e_{11}(1)=e_{11}(2)=e_{33}(2)=\mu_3[\mu_1(\mu_1+3\mu_2)+\nu_1(3\mu_1+\mu_2)]/2c^2(\mu_1+\mu_2+2\nu_1),$$

$$b_{12}(3)=e_{11}(3)=[\nu_1(\mu_1+\mu_2)+2\mu_1\mu_2]^2/c^2(\mu_1+\mu_2+2\nu_1)^2,$$

$$d_{11}(1)=c_{ik}(l)=f_{ik}(l)=0;$$

the remaining coefficients are obtained by interchanging the indices 1 and 2.

In the above equations μ_1, μ_2, and μ_3 are the "partial mobilities" of the electrons as defined in Eq. (3), $\nu_1(=\nu_2)$ and ν_3 are the mobilities of the holes, and λ_{ik} is the conductivity tensor.

It should be noted that in Eq. (12), $\lim[R_{ik}(l)/H]=r_{ik}(l)$ as $H\to 0$, so that $r_{ik}(l)$ is in fact the Hall coefficient. Similarly $q_{ik}(l)$ is the magnetoresistance coefficient.

IV. COMPARISON WITH EXPERIMENT

A. Pure Bismuth

Equations (12) and (13) express the galvanomagnetic effects as functions of H in terms of the "partial mobilities" μ_1, μ_2, μ_3 and $\nu_1(=\nu_2)$, ν_3 and the number of electrons and holes $N=P$. We will consider these quantities as temperature-dependent parameters. It is reasonable to assume that the dependence of the effective masses on temperature can be neglected. The temperature dependence of the mobilities will then be due entirely to the relaxation time [Eq. (3)] and the ratios $\mu_1:\mu_2:\mu_3$ and $\nu_1(=\nu_2):\nu_3$ will be independent of temperature. The parameters subject to this restriction have been determined at 80°K and 300°K, so as to obtain the best fit of the experimental [Table I] and theoretical [Eqs. (14)] values of the conductivities and the weak magnetic field coefficients. The values of the parameters so obtained are given in Table II. From a comparison of the calculated and the experimental values in Table I, it will be seen that a reasonable fit can be obtained.

The same values of the parameters have been used to calculate the dependence of the galvanomagnetic effects on the magnetic field strength [Eqs. (12) and (13)]. Comparison between calculated and experimental values are given in Figs. 1, 2, and 3.

It should be noted that the determination of the parameters from the weak magnetic field coefficients, as described above, leaves the possibility of interchange of the values of μ_1 and μ_2. This is seen immediately from Eqs. (14), which are symmetrical in μ_1 and μ_2. A positive assignment can however be made from the strong field results. In Figs. 1, 2, and 3 interchange of directions 1 and 2 leads to interchange of the theoretical curves and to disagreement between theory and experiment.

B. Tin-Doped Bismuth

Some of the results for tin-doped bismuth crystals are given in Figs. 4, 5, and 6. The main features of these curves follow naturally from the proposed model, if we make the additional assumption that the tin impurities introduce acceptor levels near the top of the valence band. Consideration of such an energy scheme will show that at intermediate temperatures (kT of order of magnitude of the band overlap) the introduction of acceptor levels will cause a reduction in the number of electrons and an increase in the number of holes. At low temperatures and at high temperatures the effect of the acceptor levels is small.

In the proposed model the mobility of the electrons in the direction of the trigonal axis (μ_3) is much larger than the mobility of the holes (ν_3), (see Table II). Accordingly the resistivity in this direction is very sensitive to the number of conduction electrons. This explains the pronounced maxima in the curves of Fig. 4. On the other hand, in the direction perpendicular to the trigonal

TABLE II. Values of the parameters used in the calculations. $N=P$ is the number of electrons or holes per unit volume; μ_1, μ_2, μ_3 the electron mobilities and $\nu_1(=\nu_2)$, ν_3 the hole mobilities in directions corresponding to the principal axes of the energy ellipsoids All quantities in cgs units.

	300°K	80°K
$N,P\times 10^{-18}$	2.2	0.46
$\mu_1\times 10^{-6}$	9.5	167
$\mu_2\times 10^{-6}$	0.24	4.2
$\mu_3\times 10^{-6}$	5.7	100
$\nu_1,\nu_2\times 10^{-6}$	2.3	37
$\nu_3\times 10^{-6}$	0.62	10

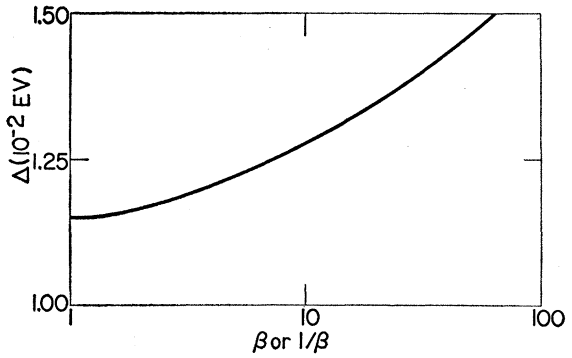

FIG. 7. Calculated overlap of conduction and valence bands in bismuth as a function of assumed ratio β of densities of states of electrons and holes. The curve is symmetrical about the ordinate $\beta=1$.

axis, the electron mobility $(\mu_1+\mu_2)/2$ and the hole mobility (ν_1) are of the same magnitude and a pronounced maximum cannot be expected. It will be seen that this agrees with the observed facts. The fact that in the intermediate temperature range the number of electrons is decreased by the addition of tin, while the number of holes is increased, also gives a qualitative explanation of the change in sign of the Hall effect as illustrated in Fig. 5, and of the inflection in the magnetoresistance curves, given in Fig. 6. The behavior of the curves at the lower temperature is of course also determined by impurity scattering.

We have not succeeded in placing the above qualitative arguments on a quantitative basis. In order to carry through such an analysis, measurements are required on two differently oriented samples for each impurity content. In practice it has proved impractical to obtain two samples with nearly equal impurity concentrations, the allowed variation being very small because of the high sensitivity of the effects to changes in impurity concentration.

V. DISCUSSION

A quantity of interest is the amount of overlap (Δ) of the valence and conduction bands. Although the above analysis gives a value for the number of electrons and holes $(N=P)$, calculation of Δ would also require knowledge of the density of states, i.e., *absolute* values for the effective masses. Alternatively, it can be shown that, if the temperature dependence of the overlap is neglected, knowledge of N at two different temperatures and of the *ratio* (β) of the density of states in the conduction band and the valence band suffices to determine Δ. Using tables of the Fermi-Dirac functions[20] and the values of $N=P$ given in Table II, we have calculated Δ for different assumed values of β. The results are given in Fig. 7. It will be seen from this figure that Δ is rather insensitive for variations of β, and even though the actual value of β is not known, an estimate of $\Delta=0.012$ ev seems reasonable.

The most convincing evidence as to the validity of the proposed model is the ability of the theory to predict the dependence of the galvanomagnetic effects on magnetic field correctly, see Figs. 1, 2, and 3. It should be emphasized that the values of all six parameters used in calculating the theoretical curves have been obtained from the weak magnetic field coefficients only the assignment of μ_1, and μ_2 being left open (see Sec. IV.A).

At very strong magnetic fields the theory as given here is no longer satisfactory. This theory predicts for the case $N=P$ a Hall effect proportional to H and a transverse magnetoresistance proportional to H^2 as $H\to\infty$ [in Eqs. (12) and (13), $c_{ik}(l)=f_{ik}(l)=0$ if $N=P$]. On the other hand, the theory predicts longitudinal magnetoresistance which does saturate [in Eq. (13), $d_{ik}(l)=f_{ik}(l)=0$]. Measurements of Kapitza up to 300 kilo-oersteds show that the longitudinal magnetoresistance saturates, and in fact the above theory reproduces the curves given by Kapitza[1] and those by Stierstadt[2] quite well. On the other hand the transverse effects are found to increase linearly with H at high magnetic fields[1] in contrast with the theory. This behavior, which seems to be typical for other metals as well,[1] remains unexplained. Measurements of the Hall effect at strong magnetic fields and low temperatures[4,5] show a complicated and irreproducible behavior, and no definite conclusions can be drawn from them.

From an interpretation of the de Haas-van Alphen effect in bismuth, Shoenberg[17] has arrived at a model for the conduction band similar to the one proposed here. Shoenberg does not take the contribution of the valence band into account. The ratios of the effective masses of the conduction band ellipsoids calculated by Shoenberg are 0.063:106:1 while we obtain 0.60:24:1.

The model proposed here is the simplest one giving reasonable agreement with experiment. A model in which the valence band is described by three ellipsoids and the conduction band by one ellipsoid is incapable of explaining the observed facts. Obviously more complicated models involving more parameters, such as a three-ellipsoid model both for the valence and conduction band or a three-ellipsoid model in which the ellipsoids are rotated about the binary axis, are possible. At this stage it does not seem fruitful to speculate about such refinements.

ACKNOWLEDGMENTS

We are indebted to Dr. Joseph Jaffe and Mrs. Ilana Levitan of this Institute, for carrying out the spectroscopic analysis of the tin-doped bismuth crystals.

[20] J. McDougall and E. C. Stoner, Trans. Roy. Soc. (London) **237**, 67 (1939).